Biochimica et Biophysica Acta, 554 (1979) 204—226

BBA 78404

DIVALENT CATIONS COOPERATIVELY STABILIZE CLOSE MEMBRANE CONTACTS IN MYELIN

VICKI MELCHIOR, C.J. HOLLINGSHEAD and D.L.D. CASPAR

Structural Biology Laboratory, Rosenstiel Basic Medical Sciences Research Center, Brandeis University, Waltham, MA 02154 (U.S.A.)

(Received December 18th, 1978)

Key words: Myelin; Compaction; Ca^{2+}; Intramembrane particle; Electron density profile

Summary

Intact nerve myelin compacts to a dehydrated structure of closely apposed membranes when exposed to isotonic solutions at least 10 mM in calcium or tetracaine. The repeat period of the membrane pair in the compacted structure measured by X-ray diffraction is about 126 Å in both central and peripheral mammalian nerve myelins whereas the normal periods are about 158 and 178 Å, respectively. The electron density profile of compacted myelin shows an asymmetric membrane unit with thickness similar to that of the symmetric bilayer of flocculated myelin lipids. The centrosymmetrically averaged myelin membrane profile is similar to that of the lipid bilayer except at the surface where residual protein is concentrated. Dispersions of extracted total myelin lipids flocculate under similar conditions to those causing myelin compaction, indicating that similar forces act in both processes. Compaction is always accompanied by lateral segregation of intramembrane particles out of the close-packed domains. Lateral displacement of intramembrane proteins from compacted domains can be driven by the attraction of the lipid surfaces for each other. Rates of compaction vary with compacting reagent, concentration, tissue, and temperature, and probably reflect the permeability of the tissue. Extensive compaction by calcium or tetracaine leads to disruption and vesiculation of the spirally wrapped myelin membranes.

Introduction

Divalent cations induce close contact of cell membranes [1—3] and acidic lipid bilayers [4]. Close contact necessarily precedes membrane fusion but does not necessarily lead to it. Regions of cell membranes in close contact normally

appear to be depleted of intramembrane particles [1,3,5,6]. The resemblance between ion effects on acidic lipids and those on cell membranes has prompted recent studies relating divalent cation-induced lipid flocculation, surface charge neutralization, and vesicle fusion [7–9].

Stacked membranes of nerve myelin and multilayers of myelin lipid constitute a comparative system for assessing the role of lipid-lipid interactions in close approach of membrane surfaces. Palmer and Schmitt [4] observed by X-ray diffraction an abrupt decrease in bilayer separation of myelin lipid emulsions as calcium content was increased above a critical level. The compacted lipid structure had a repeat period of 67 Å which corresponds to close contact of bilayer surfaces. Calcium above 10 mM induces compaction in the myelin sheath of intact nerves to form a structure with repeat period about 126 Å [10]. The repeating unit in this 126 Å period is a pair of symmetrically related membranes each 63 Å thick. This packing thickness is slightly less than that of a myelin lipid bilayer compacted by calcium. Treatments that lower water activity also lead to close packing of myelin membranes [11]. Compaction by any treatment appears always to be coupled with lateral segregation of intramembrane particles out of the close-packed layers and into particle-enriched regions that have a normal or slightly expanded repeat period [12].

We have carried out a detailed study by X-ray diffraction and electron microscopy of the actions of calcium and tetracaine on the intact nerve sheaths of central and peripheral nerves, and a comparison of their actions on purified myelin lipids. The correlation of electron microscopy with diffraction forms a basis for interpreting the periodicities measured by X-ray diffraction in terms of the structures seen in the microscope. Conversely, X-ray patterns provide a direct control for distinguishing artefacts that may be produced during sample preparation for microscopy. The objective of this study has been to characterize the molecular interactions involved in close packing myelin membranes and to delineate the structure of the membrane unit in the close-packed array.

Materials and Methods

Tissues and tissue preparation

Specimens. Myelinated tissues examined by X-ray diffraction included: sciatic nerves from mouse, hamster, frog, and gerbil; bovine intradural roots; white matter from bovine and calf brain (pons and medulla); and optic nerves from calf and hamster. Freshly dissected tissues were bathed in isotonic Ringer's or buffered saline solutions containing alkaline earth cations or tetracaine hydrochloride. Isotonicity was maintained in the solution by reducing the concentration of sodium chloride. Tissues for diffraction were bathed for periods from 15 min to 5 days, then mounted in quartz capillaries for X-ray exposure. Studies at lowered or elevated temperatures were performed by bathing nerves in calcium-containing solutions at 4 or 37°C, then mounting them in capillaries for 20–30 min X-ray exposures at room temperature. The specimens used for freeze-fracture and thin-section electron microscopy were calcium- and tetracaine-treated mouse sciatic nerves and calcium-treated calf white matter.

Ringer's and saline solutions. Normal mammalian Ringer's solution con-

tained 145 mM NaCl, 6 mM KCl, 2 mM $CaCl_2$, and 2 mM $MgCl_2$, buffered to pH 7.4 with 1.5 mM $NaHCO_3/NaH_2PO_4$ buffer. Physiological saline for mammalian tissues contained 156 mM NaCl, buffered with 10 mM Tris-HCl, Ringer's buffer, or phosphate buffer. Amphibian sciatic nerves were bathed in phosphate- or $NaHCO_3/NaH_2PO_4$-buffered physiological saline (120 mM NaCl).

Kinetics of calcium transformation. Freshly dissected nerves were mounted under slight tension in quartz capillaries open at both ends, and bathing solution was dripped continuously through the capillary. Successive short X-ray exposures were made without disturbing the position of the nerve. Mouse sciatic nerves were used to study the dependence of the rate of calcium-induced compaction on temperature, ion concentration, and additions of dimethylsulfoxide. A few kinetics studies were performed on hamster sciatic nerve, intact and desheathed frog sciatic nerve, and calf white matter in order to examine tissue-specific differences.

Reversibility. Diffraction studies of reversibility were carried out only on mouse sciatic nerves compacted by calcium at room temperature. Normal Ringer's solution, calcium-enhanced Ringer's solution, then normal Ringer's solution were successively dripped through the capillary without altering the position of the nerve in the X-ray beam.

Tetracaine, barium, magnesium and manganese. The effects of tetracaine hydrochloride were studied on mouse sciatic nerve at room temperature over the concentration range 0.5—20 mM tetracaine. $MgCl_2$, $BaCl_2$, and $MnCl_2$ were studied only at 33 mM at room temperature with intact and purified calf white matter and with mouse sciatic nerve.

Purification, analysis, and preparation of lipids

Central nervous system. Myelin was purified from bovine lower brain stem by a modification of the method of Norton and Poduslo [13]. Purified myelin was suspended in one part water and extracted with 19 parts chloroform/methanol (2 : 1) by the procedure of Folch et al. [14]. Basic protein was precipitated with KCl [15]. Proteolipid protein was removed by passing the concentrated extract twice through a Sephadex G-25 column, equilibrated according to the solvent sequences suggested by Rouser et al. [16]. The final lipid extract contained less than 0.33% protein by weight.

Peripheral nervous system. Intradural roots dissected from the caudal segments of adult cattle spinal cords were homogenized in 0.32 M sucrose, and the myelin fraction was purified by the same procedure used for central nervous system tissue. Purified peripheral nerve myelin was extracted by the Folch procedure. Repeated washing of the lipid extract with KCl reduced the protein content to less than 0.75% protein by weight. Water-washed lipid extracts from both central and peripheral myelin were dried under vacuum, taken up in chloroform, and stored under N_2 at —20 or —60° C.

Lipid extract composition. Lipid extracts were assayed for dry weight, protein (by Folin-Lowry assay) [17], phosphorus [18], cholesterol [19], and cerebroside [20]. Average compositions for central and peripheral nerve myelin lipids are given in Table I.

Lipid dispersions. Lipids were dried under vacuum and then under N_2 for several hours. Multilayered vesicles were formed in Tris- or phosphate-buffered

TABLE I

AVERAGE COMPOSITION OF EXTRACTED MYELIN LIPIDS

n, number of determinations

Class	Bovine brain myelin lipids		Bovine intradural root myelin lipids	
	n	Weight fraction	*n*	Weight fraction
Cholesterol	4	0.211	9	0.238
Galactocerebrosides	4	0.252	5	0.146
Phospholipids	4	0.520	15	0.628
		0.983		1.012

physiological saline or normal Ringer's according to the procedure outlined by Kinsky [21]. Dispersions were allowed to swell for 6—12 h before use. Concentrations of divalent ions, Me_2SO, and tetracaine required for rapid flocculation of lipid were identical whether the agents were added to swollen vesicle dispersions or were present in the initial swelling solution.

Dispersions and flocculates were concentrated for X-ray diffraction by centrifuging samples at 131 000 × *g* into conical tip Beem embedding capsules (Ernest F. Fullam, Inc., Schenectady, NY) held in epon resin adaptors fitted to the Beckman SW27 rotor buckets. Buckets were flushed with nitrogen and sealed prior to centrifugation. The concentrated samples were packed into quartz capillaries either directly or in yokes made by trimming the Beem capsule. Lipid specimens for X-ray diffraction were found to be stable for at least a week when stored at 4° C.

X-ray diffraction

Diffraction patterns for accurate measurement of intensities and line profiles were recorded on packs of four Ilford Industrial-G X-ray films using double mirror or mirror monochromator focusing cameras with CuKα radiation from an Elliot rotating anode X-ray tube. The order-to-order resolution of these point-focus cameras was approximately 0.001 $Å^{-1}$. The exposure time for detecting weak reflections from nerve and lipid specimens out to about 15 Å spacing was approximately 24 h. Kinetics of compaction in nerve specimens were followed by recording successive short exposures using a single mirror camera with the line source of a Philips fine-focus X-ray tube. With this line-focus camera diffraction patterns out to 30 Å spacing could be recorded in 15—30 min. Diffraction patterns from nerves treated at lowered or elevated temperatures prior to the X-ray exposure were recorded only once at room temperature. Absorbances of X-ray photographs were measured on a 50 μm square grid with an Optronics P-1000 densitometer. For the patterns from the point-focus cameras, absorbances were integrated along arcs. Background was defined by fitting a smooth curve to the intensities measured between the Bragg reflections. This background includes incoherent scatter from disordered parts of the specimen, camera background and film fog. The intensity of the Bragg reflections from the coherently diffracting periodic structure was determined by integrating the area under the diffraction maxima after background

subtraction. By measuring the absorption of consecutive films in the pack, the weak reflections were scaled to the strong ones.

Electron microscopy

Myelinated nerve tissue was immersed in Ringer's solution plus 33—100 mM calcium or 10—20 mM tetracaine for periods from 15 min to 24 h at room temperature or 37°C. Treated nerves and controls were fixed for thin sectioning in 2.5% glutaraldehyde, followed by 1% OsO_4. Ringer's solution and calcium or tetracaine were maintained throughout the fixation. Fixed specimens were rinsed briefly in buffer, dehydrated through a graded series of alcohols to propylene oxide, and embedded in epon. Thin sections cut on a diamond knife were stained with uranyl acetate and lead citrate.

For most freeze-fracture experiments, control tissues and treated specimens were bathed, without fixation, in solutions containing 20% glycerol for 2 h. Direct comparisons were made between these specimens and similar specimens frozen without cryoprotectants. Cryoprotection with glycerol was omitted for nerves treated with calcium in the presence of dimethylsulfoxide. Small pieces of nerve to be frozen were mounted on cardboard disks and immersed in a slush of Freon 22 at liquid nitrogen temperature. Samples were fractured at —116°C in a Balzers BAF301 according to standard techniques. After storage overnight in methanol, the replicas were cleaned in Clorox and mounted on uncoated grids. All observations were made on a Philips 301 electron microscope.

Results

Repeat period

Repeat periods of 126 ± 2 Å are found by X-ray diffraction for the compacted phases of all mammalian central and peripheral nerves treated with calcium. Barium and magnesium, tested on calf white matter, and tetracaine hydrochloride, tested on mouse sciatic nerve, produce similar compacted phases with a 126 Å repeat. Calcium-compacted frog sciatic myelin has a period of 117—120 Å. Native periods measured for these specimens are about 154—158 Å for mammalian central nerves, 178—182 Å for mammalian peripheral nerves, and 169—171 Å for frog sciatic.

The repeat periods of the calcium- and tetracaine-compacted phases are invariant under the range of experimental conditions tested. For calcium, these include exposure to concentrations of 5—100 mM at temperatures of 4—37°C for periods from 30 min to 5 days. Mouse sciatic nerves were exposed to 10—20 mM tetracaine for periods from 15 min to 24 h at room temperature.

Measurements of repeat periods have also been made from micrographs of

Fig. 1. (a) Myelin sheath of mouse sciatic nerve immersed for 3.5 h at 37°C in buffered Ringer's solution containing 33 mM $CaCl_2$, fixed for 1 h in OsO_4, and embedded in Epon. The bilayers in the compacted domain are continuous with those in the normal period array (X359 000). (b) Mouse sciatic myelin immersed in buffered Ringer's solution plus 0.1 M $CaCl_2$ for 5 h at 37°C, fixed in OsO_4, and embedded in Epon. A portion of the compacted array has looped back on itself. In the particle-enriched domain, membrane pairs have split apart at the cytoplasmic boundary (X117 000).

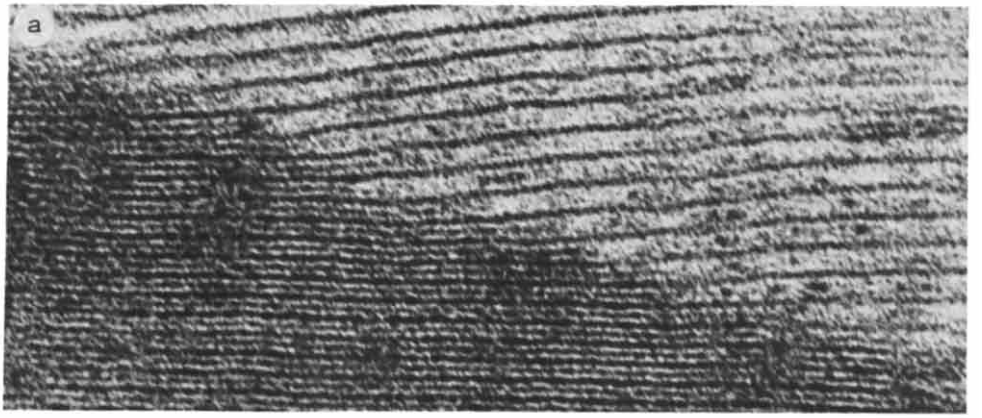
a

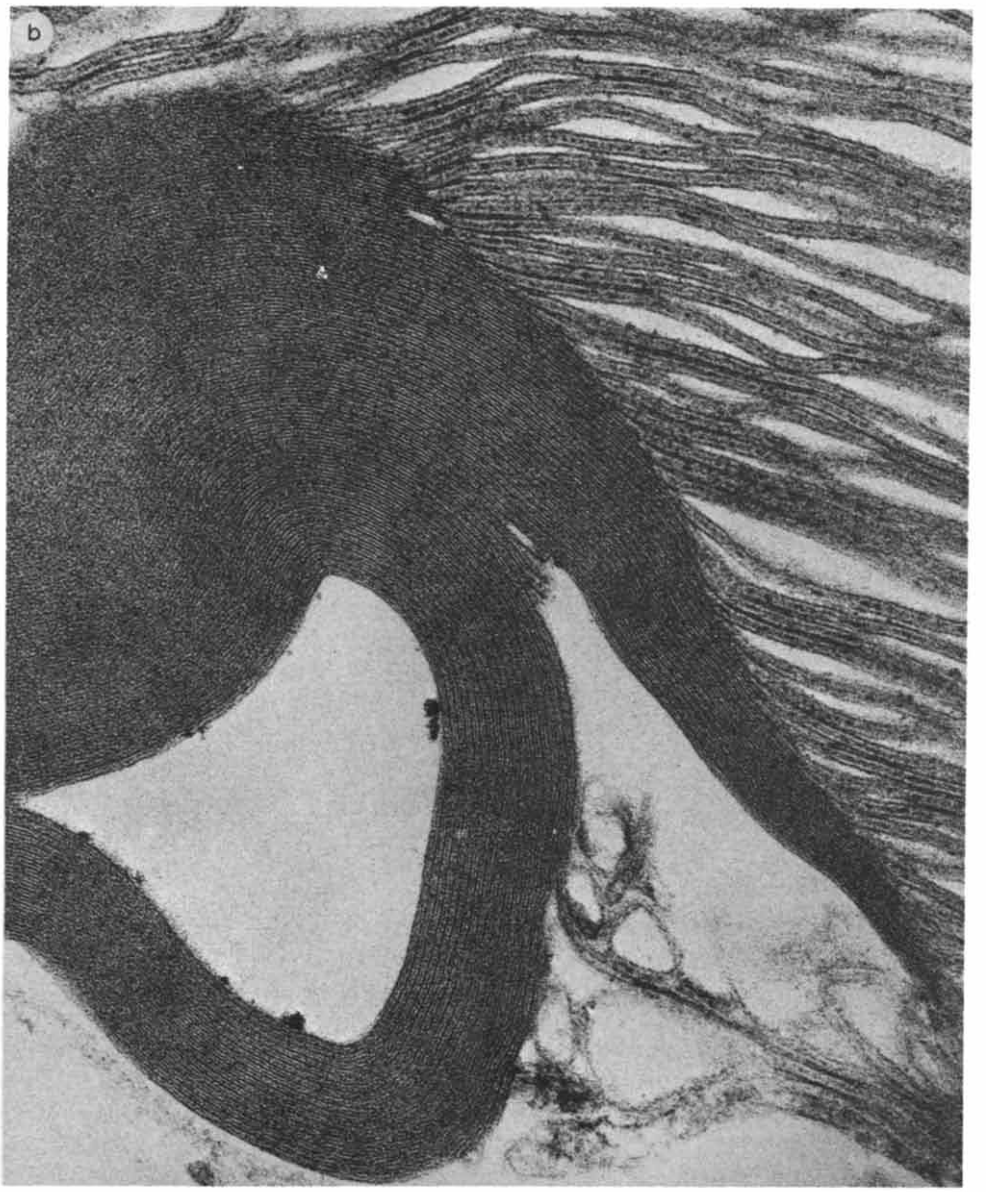
b

thin-sectioned and freeze-fractured tissue. Freezing with cryoprotectants preserves the lattice period. The 125 Å ± 10 Å repeat period of compacted arrays measured from micrographs of cross-fractured specimens corresponds within the accuracy of the measurements to X-ray diffraction spacings. Non-uniform shrinkage is induced in both native and compacted phases by the fixation and embedding treatments for thin sectioning.

Morphology

Continuity of membrane bilayers between compacted and normal period arrays is evident from thin sections of osmium-fixed specimens (Fig. 1) and from replicas of freeze-fractured nerves (Fig. 2). The smooth fracture faces and the particle-enriched regions look similar in all myelins compacted by calcium, tetracaine, and dehydrating treatments [12]. Both compacted and particle-enriched domains retain the asymmetric staining pattern of alternating major and minor dense lines (Fig. 1) found in thin-sectioned, intact myelin.

Fracture faces of myelin membranes normally show particles that are evenly distributed (Fig. 3b and Refs. 12 and 22). The particle segregation caused by compacting treatments is apparent in the absence of cryoprotectants (Fig. 3a). Particle segregation occurs under conditions that induce the formation of compacted arrays detected by X-ray diffraction and not, therefore, as a by-product of the preparations for freeze-fracture. Glycerol itself induces a transient particle segregation in myelin during the first hour of exposure but this effect is reversed after 2 h (Fig. 3b). Glycerol prevents ice damage to the tissue (cf. Figs. 2b and 3a) while preserving the particle segregations caused by divalent cations.

Micrographs of thin-sectioned and cross-fractured specimens treated with calcium or tetracaine under conditions producing extensive compaction show disruption of the continuity of the spiral wrapping (Figs. 1b, 4 and 5). The sheath structure is often fragmented into vesicles or looped back in whorls that appear to have formed by fusion of multilayer domains. Some of this reorganization may occur during the preparative treatments for electron microscopy, but controls without added divalent cations do not show similar damage.

Separation or particle-enriched membranes at the major dense line shown in Fig. 1b is the result of altered interactions at the cytoplasmic boundary in calcium- or tetracaine-compacted myelin during osmium fixation. Splitting at the cytoplasmic boundary is not observed in similarly fixed Me_2SO-compacted myelin, in normal controls, or in glutaraldehyde-fixed calcium or tetracaine-treated myelin.

Conditions for compaction

Successive stages of transformation induced in mouse sciatic myelin by buffered 0.1 M calcium at room temperature were studied by following the changes in the X-ray diffraction pattern. The sheath structure is transformed progressively until the reflections from the native phase are barely perceptible and the reflections from the 126 Å compacted phase reach a constant intensity. This stage of compaction is reached after 20—22 h at room temperature. The 126 Å phase is stable for 4—5 days. Eventually, the odd orders disappear [10],

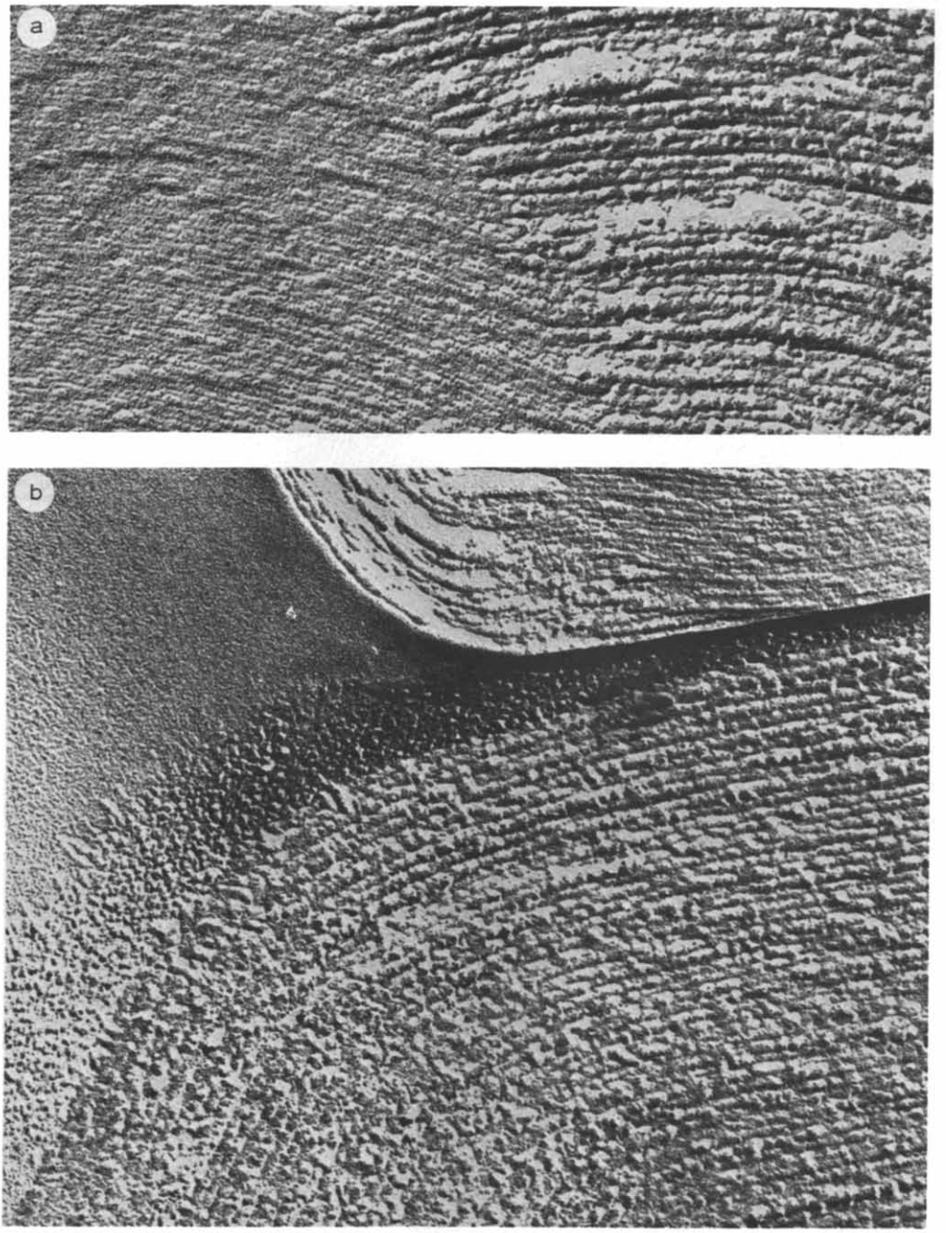

Fig. 2. Freeze-fracture replicas of mouse sciatic myelin immersed for 24 h at room temperature in buffered Ringer's solution containing 33 mM $CaCl_2$, with 20% glycerol added for 2 h before freezing. (a) The continuity between a compacted and a normal domain is seen in cross-fracture (×190 000). (b) An en face view shows the boundary between the smooth and the particle-enriched regions, which is characterized by elongated particles oriented perpendicular to the border (×200 000).

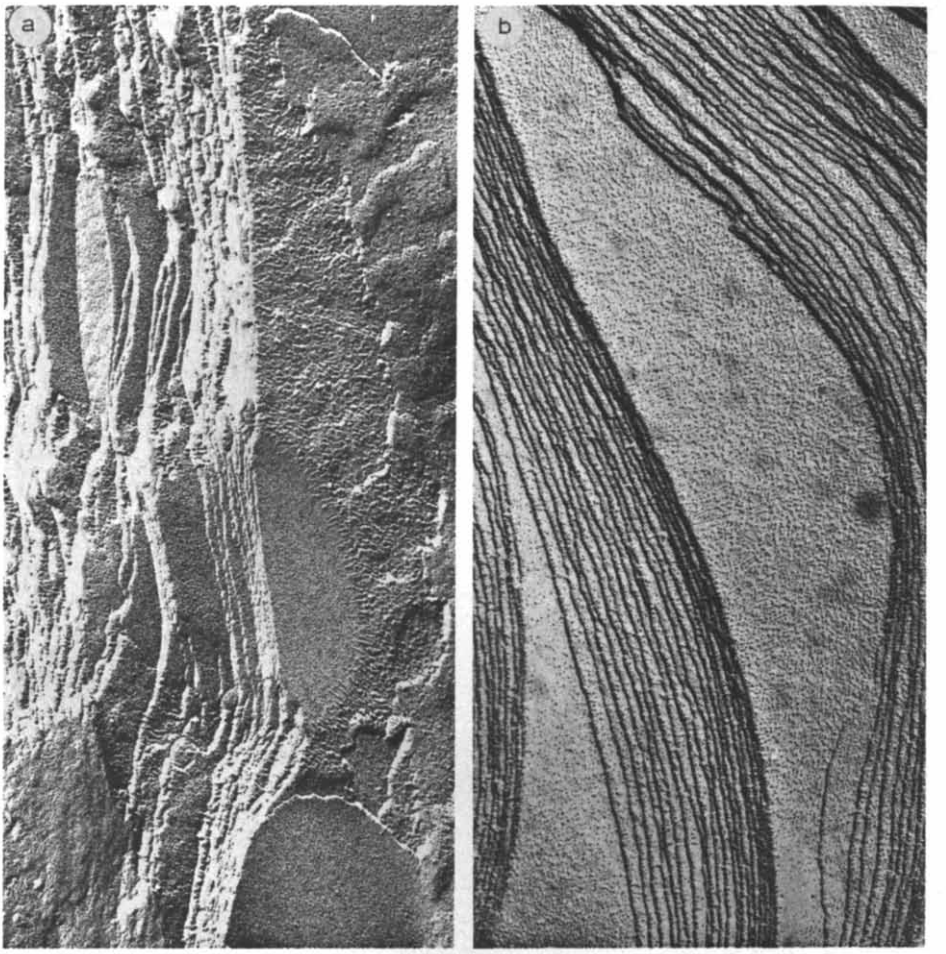

Fig. 3. (a) Freeze-fracture replica of mouse sciatic myelin maintained in normal Ringer's solution plus 33 mM $CaCl_2$ for 2.5 h at 37°C, then frozen without cryoprotection. The smooth domains are apparent in the upper left, middle, and lower right regions of the micrograph, and border particles surround the smooth domain in the center. This specimen is a control for glycerol-induced artefacts, demonstrating the same particle segregation without cryoprotectant as seen in Fig. 2b with glycerol. (b) Mouse sciatic nerve maintained in normal Ringer's solution for 3.5 h at 37°C, then in Ringer's solution containing 20% glycerol for 2 h. This control nerve demonstrates that the particles in the fracture faces of myelin membranes are uniformly distributed after 2 h exposure to glycerol (×77 000).

indicating the formation of an array of symmetric bilayers with half the repeat period of the asymmetric membrane pairs.

The same stages of compaction appear to occur for myelins compacted by all alkaline earth cations and tetracaine, but the kinetics differ with the compacting reagent, the tissue, reagent concentration, and temperature. Diffraction patterns from tetracaine-treated myelin in late stages of compaction show the 126 Å phase plus several broadened reflections from an expanded array with repeat period 220—260 Å. This expanded array is presumed to be formed from the membranes in the particle-enriched domains.

The compaction of myelin by calcium and tetracaine resembles a phase

Fig. 4. A freeze-fracture replica of myelin immersed for 24 h at room temperature in buffered Ringer's solution containing 33 mM $CaCl_2$, with 20% glycerol added for the final 2 h. The sheath structure is fragmented and looped back in whorls (×76 000).

transition. The same final stage is reached provided that the concentration of these reagents exceeds a critical threshold. The rate of compaction increases, however, with increasing concentration.

The threshold for calcium-induced compaction is about 10 mM in mouse sciatic nerve and about 5—7 mM in bovine white matter. The threshold concentration is independent of temperature over the range 4—37°C. Inclusion of 5—8% Me_2SO in the medium lowers the threshold for compaction of sciatic nerve by calcium to about 5 mM. Me_2SO alone at these concentrations produces no detectable changes in the myelin diffraction pattern.

Tetracaine compacts mouse sciatic myelin at a threshold of about 10 mM. At

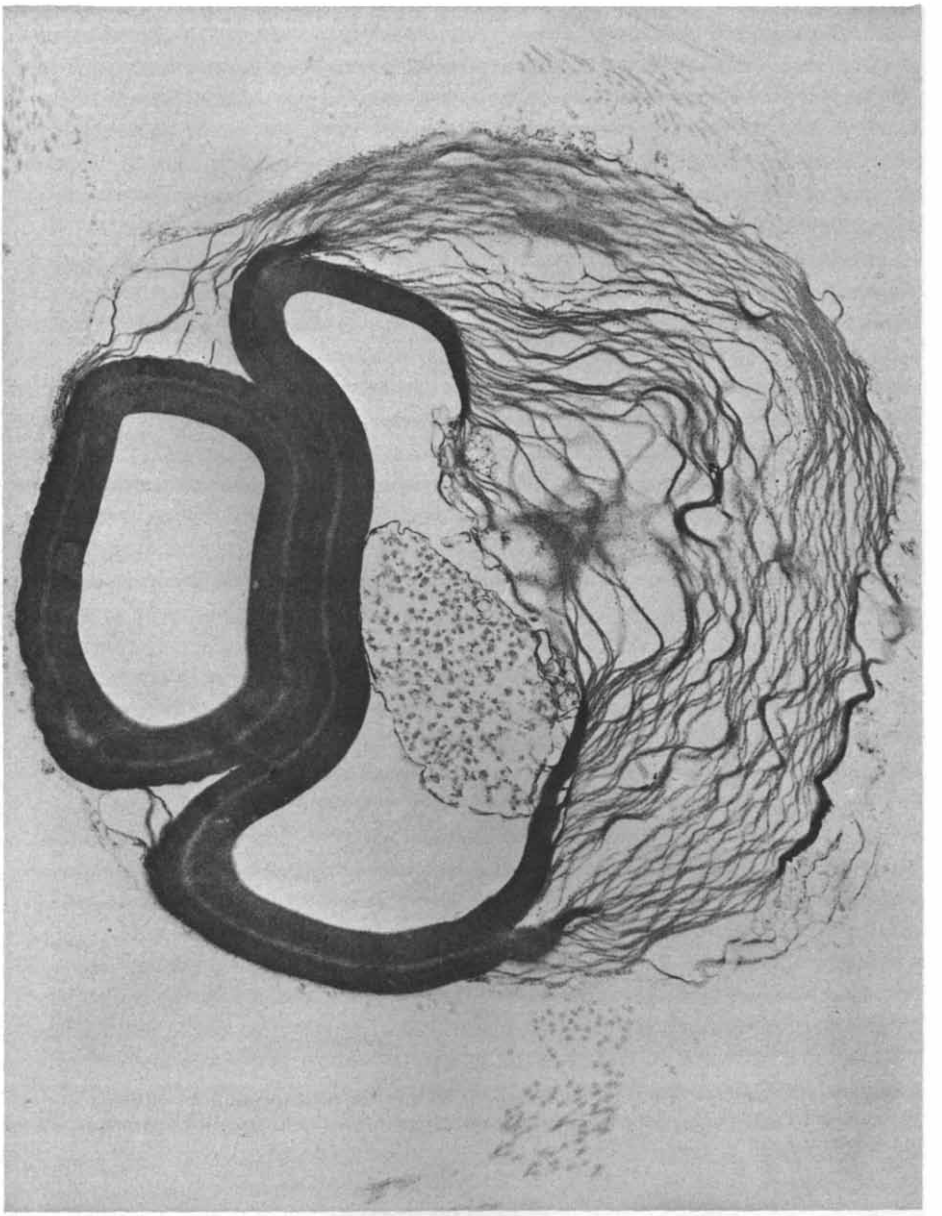

Fig. 5. Myelinated axon in mouse sciatic nerve that has been immersed for 5 h at 37°C in buffered Ringer's solution supplemented with 0.1 M $CaCl_2$. The sheath has become convoluted and vesiculated with disruption of the spiral geometry (×20 000).

concentrations of 2—7 mM, it induces formation of at least two new phases with repeat periods larger and smaller, respectively, than normal. The structures formed at low tetracaine concentrations have not been characterized.

Kinetics

The rate of myelin transformation by calcium is both temperature and

concentration dependent. Elevation of temperature from 4 to 37° C produces a 25-fold increase in the rate of compaction by 33 mM calcium. The rate increases 20—25 fold when calcium concentration is raised from 10 to 100 mM. Addition of 5—8% Me_2SO approximately doubles the rate of compaction by 33 mM calcium at room temperature.

The sequence of events during the early stages of transformation varies with ion concentration. With 33 mM calcium, faint reflections from the new phase appear after 75 min at room temperature, and diffraction from the native phase disappears slowly over the next 12—18 h. With 100 mM calcium, the intensity of diffraction from the native phase falls by 90% within the first 45—90 min, while reflections from the compacted phase first appear after about 2 h.

When the formation of the compacted phase proceeds slowly, as with lower concentrations of calcium, weak diffraction from an intermediate phase with repeat period about 147 Å is often observed in mammalian sciatic nerves Other weak reflections of variable spacing may appear at the later stages of transformation. The structures giving rise to these weak, transient reflections were not characterized.

Electrophysiological studies have shown that the perineural connective tissue sheath of frog sciatic nerve is a permeability barrier to calcium [23,24]. Paired sciatic nerves, one intact and one desheathed, were exposed to 33 mM calcium at room temperature. Detectable diffraction from the 118 Å compacted phase appeared after 75 min with the desheathed nerve but only after 24 h with the intact control.

The kinetics of transformation also depend on the tissue and the compacting reagent. Calf white matter treated with 33 mM calcium at room temperature is transformed twice as rapidly as mouse sciatic nerved treated identically. Micrographs of mouse sciatic nerves treated with 20 mM tetracaine for 15 min show a stage of compaction corresponding to that seen after calcium treatment for 18—24 h. Similarly, the time required for odd orders in the X-ray patterns of the 126 Å phase to disappear is 2 h with 20 mM tetracaine and longer than 4—5 days with 0.1 M calcium.

Reversibility

When limited compaction has occurred, the normal diffraction pattern is restored within 15 min by returning a calcium-treated nerve to Ringer's solution, but the initial diffracting power is not fully recovered. Micrographs of calf white matter treated for 6 h in 33 mM calcium and returned to Ringer's prior to fixation show membrane arrays with staining patterns and repeat periods similar to normal controls, but with increased disorder in the membrane stacking.

When transformation has proceeded to the point that only diffraction from the compacted phase is observed, immersion in normal Ringer's leads to the formation over several hours of an expanded phase with repeat period 3—5 Å greater than untreated controls. Diffraction from the expanded phase consists of a few weakened broad reflections.

Compaction of purified myelin

Myelin purified from bovine and calf white matter has a repeat period 150—

153 Å in water and 152–154 Å in Ringer's solution. The 153 Å repeat period for the asymmetric membrane pair is about 5 Å smaller than that for intact bovine white matter. Purified myelin suspensions are precipitated by alkaline earth cations at 10 mM. Diffraction patterns of the precipitate show two phases of repeat periods 62–64 Å and 150–155 Å. The 62–64 Å phase consists of stacked bilayers whose separation approximates that of the membranes in the 126 Å repeat unit of calcium-compacted arrays in intact nerve; but the absence of odd orders for the pattern indexed on a 124–128 Å repeat means that the membranes in the precipitate of purified myelin are centrosymmetric. This symmetric compacted phase coexists with residual 150–154 Å phase at all divalent ion concentrations from 10 to 80 mM, but the proportions of the two phases vary unreproducibly.

Flocculation of myelin lipids

Dispersions of total central or peripheral nerve myelin lipids (1%, w/v) in buffered physiological saline or normal Ringer's are rapidly flocculated by 10 mM calcium. In the presence of 5–8% Me_2SO, the threshold for rapid flocculation is reduced to about 5 mM calcium. Similar rapid flocculation occurs with 2–3 mM tetracaine, with 10 mM barium, magnesium, and strontium, and with about 15% dimethylsulfoxide. The thresholds for calcium- and tetracaine-induced flocculation are in agreement with the values found by Feinstein [25] for dispersions of cephalin, phosphatidylserine, phosphatidylethanolamine, and phosphatidylinositol at similar ionic strengths.

Prior to flocculation, the lipid dispersions in Ringer's or saline solution consists of multilayered vesicles whose repeat period depends on the lipid concentration. Diffraction patterns of the lipids after flocculation show a single lamellar phase with sharp reflections extending to the fourth or fifth diffraction order of the 64–66 Å repeat. Repeat periods of 64 Å and 66 Å are found for the precipitates of lipids from central nerve myelin and from peripheral nerve myelin, respectively. These repeat periods are the same for all the cations tested; but the relative intensities of reflections from lipids flocculated by tetracaine do differ slightly from those of specimens treated with alkaline earth cations. There are no distinguishable differences among the diffraction patterns from specimens flocculated by different alkaline earth cations.

Measurement of diffraction patterns

Diffuse high angle scattering at a spacing of about 4.5 Å was observed from all myelin and hydrated lipid specimens. This broad reflection arises from the side-to-side arrangement of the hydrocarbon chains packed with liquid-like disorder. The intensity of this reflection is dependent on the amount of lipid in the X-ray beam, but the width of the reflection appears to be the same for all specimens.

The relative amounts of myelin membrane bilayers in the compacted and native period phases are estimated from the diffraction power [11] calculated from the intensity of the two sets of small angle X-ray reflections. When the compaction of calcium-treated nerves is completed, the diffracting power of the 126 Å period phase is comparable to that of the native 178 Å period phase prior to treatment.

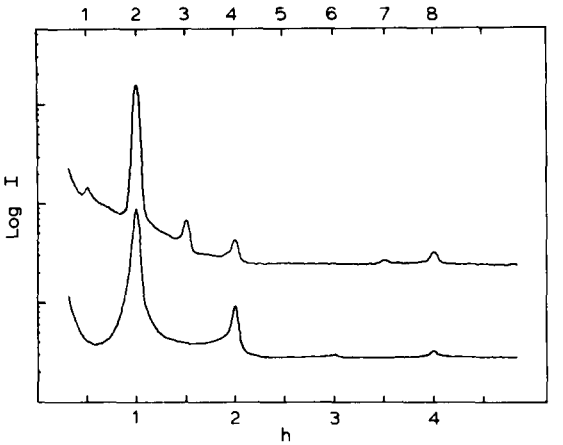

Fig. 6. Densitometer tracings of diffraction patterns used to calculate the profiles of Fig. 7. The lower diffraction pattern is from intradural root lipid flocculated in Ringer's + 8 mM $CaCl_2$. The lower scale along the abscissa marks the reciprocal, space positions of the reflections $h = 1$—4 for the unit cell a = 66 Å. The upper diffraction pattern and scale for mouse sciatic nerve compacted with buffered 0.1 M $CaCl_2$, for which the unit cell is a = 124 Å. The traces are shown to 15 Å spacing but the films show measurable diffraction to $h = 5$ (lipid pattern) and $h = 10$ (compacted phase pattern). The ordinate plots the logarithm of diffracted intensity. The traces are vertically displaced by one decade. Details of treatment are given with Fig. 7.

The width of the X-ray reflections is inversely proportional to the thickness of the coherently diffracting domains of the periodic array. Disorder in the membrane stacking limits the distance over which the scattering of successive layers remains in phase [26—28]. For control mouse sciatic nerves the intrinsic width of the second-order reflection is about 1/10 its Bragg spacing. This implies that the coherence length is about the thickness of ten membrane layers. For the compacted myelin, the reflections are somewhat sharper, corresponding to about 15 layers in a coherently diffracting domain. Diffraction patterns from calcium-flocculated myelin lipids have reflections comparable in width to those of calcium-compacted myelin (Fig. 6), indicating similar order in the layer stacking. Bragg reflections beyond 12 Å spacing have not been observed for the nerve and lipid specimens examined in this study.

The background intensity between the Bragg reflections in Fig. 6 is due in part to incoherent scattering from irregularities in the layer stacking. Density fluctuations from other parts of the nerve tissue also contribute to the diffuse small angle scattering. Background due to both extraneous and incoherent scattering was subtracted by fitting a smooth curve to the measured intensity between the Bragg reflections. Integrated coherent intensities measured for two different clacium-treated nerves differed from each other by less than the estimated experimental uncertainty in the measurements, and these measurements were therefore averaged for further analysis. Reproducible diffraction patterns were recorded from intradural root myelin lipid dispersions flocculated by calcium.

Electron density profile

The diffraction pattern from calcium-compacted myelin corresponds very closely to that from Me_2SO-compacted myelin specimens which have a repeat

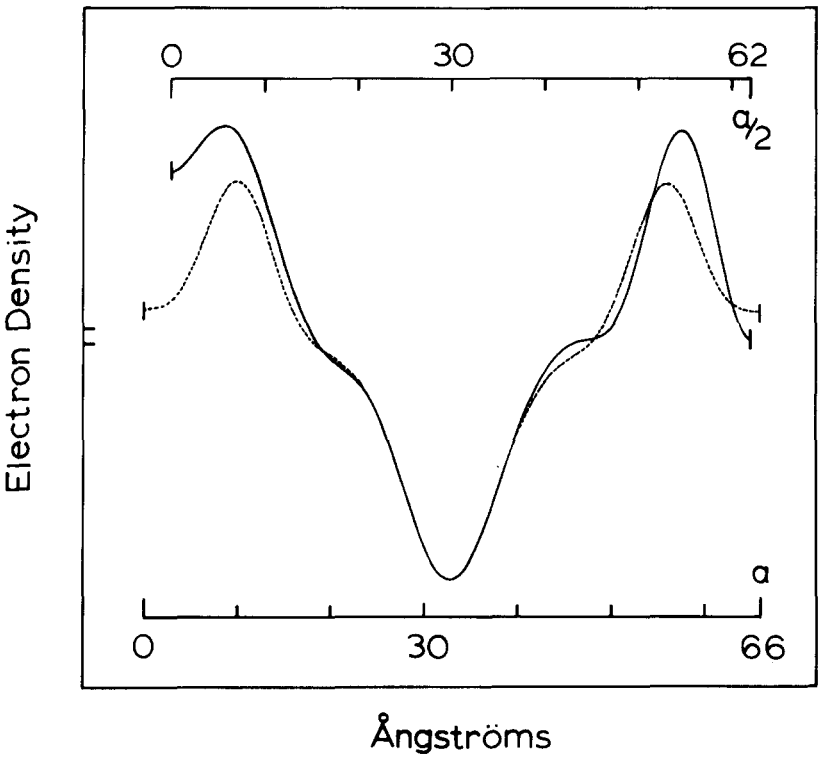

Fig. 7. Electron density profiles for calcium-compacted myelin membrane unit from mouse sciatic nerve (———) and for calcium-flocculated peripheral myelin lipids (· · · · · ·). The unit cell dimension for the membrane pair in the compacted array is a = 124 Å and for the lipid bilayer, a = 66 Å. The cytoplasmic boundary of the compacted phase, taken as the origin, is at the left and the external boundary at $a/2$ is at the right. The compacted nerve profile was taken from measurements on two nerves immersed in buffered 0.1 M calcium at room temperature for about 15 h, then exposed to X-rays for about 33 h. The lipid isolated from bovine intradural root myelin was dispersed in Ringer's, the dispersion brought to 10 mM in $CaCl_2$, and the resulting flocculum allowed to equilibrate for 5 h prior to the X-ray exposure of 41 h.

period of 126 Å. At concentrations of calcium from 10—100 mM, the repeat period of the compacted array is 126 Å ± 2 Å; in contrast, the repeat period of the Me_2SO-compacted structure decreases from 128 Å to 118 Å with increasing Me_2SO concentration in the range 10—50% [11]. The scaled intensities of the Bragg reflections from the Me_2SO-compacted arrays with slightly different periods map the continuous transform of the close-packed pair of membrane units. Since the density profile for the coherently diffracting structure is centrosymmetric, the transform is real and the phases are either positive or negative. Nodes in the transform that are fixed by the mapping uniquely define sign relations among consecutive fringes [29]. Correspondence of the relative intensities from the 126-Å period arrays induced by calcium and Me_2SO implies identical signs for the reflections in the two patterns.

Signs for the five reflections observed from flocculated myelin lipids were assigned by comparison with the phased diffraction data from lecithin-cholesterol bilayers with differing water content [30]. These signs lead to a profile for the centrosymmetric lipid bilayer that closely parallels the central

part of the compacted myelin membrane profile (Fig. 7).

The structure factors used in calculating the electron density profiles were evaluated from the integrated intensity of the coherent diffraction maxima (Fig. 6) after background subtraction. The electron density profiles for the compacted myelin and lipid specimens have been scaled in Fig. 7 to give the closest fit of their low density troughs. This choice for scaling is based on our inference, discussed below, that the central hydrocarbon layer of the compacted membranes is devoid of protein.

Discussion

Comparison of lipid and compacted myelin profiles

There is very little uncertainty in the shape of the electron density profiles (Fig. 7) calculated for the compacted myelin membrane and for the myelin lipid bilayer; there is, however, no direct way to scale the two profiles. Density profiles of lipid multilayers with defined composition can be put on an absolute scale by measuring the partial thickness of solvent and lipid and the partial specific volume of the constituents [30,31]. The chemical composition of the compacted myelin membranes cannot be determined directly since the compacted structure has not been separated from the contiguous particle-enriched membranes. Nevertheless, estimates of the partial thickness of lipid, water and protein in the close-packed membrane unit can be made by setting a plausible density scale based on interpretation of the electron micrographs.

Electron micrographs of freeze-fractured compacted myelin (Figs. 2b and 3a and Ref. 12) show smooth fracture faces like those of purified lipid multilayers. Since all the intramembrane particles have been laterally displaced from the close-packed layers, it appears that there is no significant amount of protein left within the hydrocarbon layer of these membranes. Furthermore, the central low density trough of the membrane density profile is very similar to that of the lipid. If there is no intramembrane protein in the compacted layers and if there is similar packing of the hydrocarbon chains in the pure lipid bilayer and close-packed membranes, then the central low density troughs of the two density profiles should coincide.

In making comparisons among different structures, it is important to compare profiles calculated at the same resolution. Comparing features that are sharp in one profile with those that may be blurred in the other could lead to errors in scaling. Density profiles of the compacted myelin and the lipid specimens can be compared directly since there is similar disorder in the two structures. Fitting the two low density troughs together gives a scaling in which the shoulder, identified as the steroid step, of the centrosymmetric lipid bilayer profile closely approximates a centrosymmetric average of the shoulders of the asymmetric membrane profile. Since the compacted membrane layers retain asymmetry like that of the native myelin, there is no way in which the symmetric lipid profile could coincide with the asymmetric membrane profile in both steroid step regions. If the two curves were scaled at the trough and at the peaks, the lipid density at the steroid steps would be above that of the compacted membrane; furthermore, the average density of the lipid would equal or exceed that of the membrane. The scaling shown in Fig. 7 assigns a slightly

higher average density to the membrane than to the lipid bilayer. Some protein associated with the polar groups of the membrane bilayer would account for the difference in density.

Density profiles and chemical composition

The lipid multilayer consists of lipid and water. The amount of water between lipid layers can be estimated from the distance between the polar group peaks of the density profile across the aqueous boundary. Worcester and Franks [32] established a linear correlation between the partial thickness of water and the peak-to-peak separation of neighboring layers for egg lecithin : cholesterol (3 : 2) bilayers. By this calibration, the partial thickness of water is 18.9 Å in the 66 Å unit repeat of the myelin lipid multilayer. The corresponding volume fraction of water is about 29%. Calculation of the average electron density of the hydrated lipid multilayer requires knowledge of the water content, the partial specific volume of the lipid, and the number of electrons/unit of mass for the average lipid composition. The value of V_L measured with a scanning dilatometer [33] for intradural root myelin lipid is 0.963 cm^3/g. With this value for the lipid partial specific volume, and with the lipid composition and water content, the average electron density of the hydrated multilayer is 0.344 $e/Å^3$.

The electron density at the middle of the bilayer averaged at the resolution of the diffraction measurements is about 0.27 $e/Å^3$. This value together with the average electron density of the lipid bilayer (0.344 $e/Å^3$) establishes an absolute density scale for Fig. 7. The average density for the compacted myelin on this scaling is 0.349 $e/Å^3$.

The similarity of the central hydrocarbon region of the lipid bilayer profile to that of the centrosymmetrically averaged membrane profile indicates that the hydrocarbon layers in the two structures have equal thickness. Assuming, therefore, that the partial thickness of the lipid in the compacted membrane unit is the same as in the lipid multilayer (i.e. 57.1 Å), the partial thickness of water plus protein in the 62 Å membrane unit is 14.9 Å. From the average membrane density of the compacted myelin and the estimated partial specific volume of the protein, the partial thickness of protein is about 2.7 Å. This thickness corresponds to a weight of protein that is 7—8% that of the lipid. Since the weight of protein in purified peripheral nerve myelin is about 33% that of lipid [34], the preceding calculations imply that compacted myelin retains 20—25% of its original protein.

Some protein must be lost from the compacted layers corresponding to the laterally displaced intramembrane particles seen by electron microscopy. These particles can plausibly be identified with at least the glycoprotein that constitutes about 50% of the peripheral nerve myelin protein [35]. The glycoprotein appears to have the properties of an intrinsic protein similar to the proteolipid protein of central nervous system myelin [36]. With this identification, an upper limit for the fraction of protein retained by the compacted layers would be about one-half the initial amount. Fitting the two profiles together by equating the shape of the trough and step regions under the assumption that the bilayers of the centrosymmetrically averaged membrane and the pure myelin lipids are the same leads to a lower limit of about 15% for

the fraction of the original protein remaining associated with the lipid head groups.

Within the range of these estimates, it is unlikely that there is much protein penetrating the hydrocarbon layer of the compacted membranes. Since asymmetry is retained without detectable intramembrane protein, the unequal steps may represent unequal distribution of cholesterol as suggested for the native membrane [37]. Furthermore, since the profiles of the compacted and native membranes are similar, the intramembrane particle protein that is displaced should have a fairly uniform cross-section extending across the membrane.

Disorder

The liquid-like arrangement of the lipid hydrocarbon chains in myelin membranes is shown by the diffuse meridional diffraction at about 4.5 Å spacing [4,38]. In model phospholipid bilayers and in prokaryotic cell membranes the hydrocarbon chains undergo a well-characterized thermal phase transition from disordered to ordered packing as the temperature is lowered through a critical temperature range [39]; the transition is signaled in the X-ray pattern by replacement of the diffuse 4.5 Å diffraction by a sharp 4.2 Å reflection [40–43]. This transition does not occur in lipid mixtures or in eukaryotic cell membranes which include appreciable amounts of cholesterol [44,45]. Normal and compacted myelin and hydrated myelin lipids all show very much the same 4.5 Å diffuse X-ray diffraction; thus, the disordered hydrocarbon chain packing is not detectably altered by changes in interactions at the membrane surface or by removal of the intramembrane protein.

Random variations in the separation of membranes or bilayers in the periodic arrays lead to fall-off in intensity of the higher angle Bragg reflections and increase in their width. The fact that the coherent reflections fade out at about 10 Å spacing (Fig. 6) implies that the variation of the layer plane separation is about 10 Å (i.e. about a 10% variation in the mean separation). The disorder in these specimens is similar to that analyzed by Nelander and Blaurock [27,28] for the myelin of frog sciatic nerve.

The effect of disorder on the density distribution calculated from the measured coherent scattering is to smear out the profile corresponding to a perfectly ordered array by averaging over the variations in position of the units. High resolution diffraction data have been obtained from well-ordered oriented multilayers of myelin lipids (Franks, N.P., unpublished results). The profile of the bilayer in the less well-ordered flocculated lipid (Fig. 7) can be obtained by convoluting the higher resolution profile with a Gaussian representing the variation in layer separation. In general, it is not possible to go the other way to recover the high resolution profile since disorder reduces the intensity of higher angle reflections below the limit of detectability. Attempts to enhance the resolution by deconvoluting for the disorder [28] introduce spurious diffraction ripples in the calculated profile due to the abrupt cutoff in the transform at the limit of detectability.

In order to reduce the series termination artefacts in our calculated profiles, the transforms have been extrapolated to about 9 Å spacing using the known thickness of the layers and the shape of the low density trough as constraints.

Unobserved reflections are assigned amplitudes below the limit of detectability with phase and relative magnitude from the extrapolated transform. Profiles calculated in this way conform to known features of bilayer structure and are in as good agreement with the measured diffraction data as are those for which unobserved reflections are taken to have zero amplitude.

Forces in myelin compaction and lipid flocculation

Compaction of myelin and flocculation of myelin lipid dispersions occur under very similar conditions. Threshold concentrations of calcium and tetracaine for flocculation of the purified lipid are about the same as those for compaction of myelin membranes. This correspondence suggests that the membrane bilayers are brought together by the same sort of forces that lead to lipid flocculation.

Bilayers containing acidic lipids form hydrated multilayers in which the equilibrium separation of the layers is determined by the balance of electrostatic repulsion and long-range electrodynamic attraction. Lowering the water activity in acidic lipid emulsions by increased osmotic or hydrostatic pressure forces the bilayers gradually closer together [46]. Shielding the charges of myelin lipids by increased concentrations of monovalent salt also gradually decreases the bilayer separation [4]. In contrast, when calcium concentration was increased above a critical level Palmer and Schmitt [4] observed an abrupt decrease in the repeat period of myelin lipid emulsions. This critical behavior implies a change of state that depends on the binding of Ca^{2+} by the acidic lipids.

Apparent association constants in the range 10^3—10^4 have been measured for the binding of alkaline earth cations to acidic lipids [47—49]. The binding energy has been attributed predominantly to the nonspecific electrostatic interaction between the divalent cations and the charged bilayer surface as described by the theory of the ionic double layer [50]. The cooperative nature of the compaction of myelin and myelin lipids implies that calcium and tetracaine are bound more strongly by the acidic groups in the compacted lipid array than by these groups in separated lipid bilayers.

Dehydration of lipid multilayers when water activity is reduced is a graded process: the lower the water activity, the smaller the water content [46]. When water activity in myelin is reduced by increasing Me_2SO concentration from 10 to 50%, increasing amounts of compacted myelin coexist with decreasing amounts of the native period structure [11]. The decrease in repeat period of the compacted structure from 128 to 118 Å in this range of Me_2SO concentration is due to decrease in solvent content. This is not a homogenous phase transition since both the proportion of myelin membranes in the compacted phase and the solvent content of this phase vary with the water activity. Calcium and tetracaine, in contrast, have an all-or-none effect. If the activity of these cations is high enough to flocculate the lipid, then most of the myelin membrane lipid will be compacted into the 126 Å period array.

Particle segregation

Correlation of X-ray diffraction measurements on the formation of compacted arrays with electron micrographs of freeze-fractured specimens estab-

lishes that close-packing of the smooth membrane layers is always coupled with lateral segregation of intramembrane particles. Particle segregation, whether produced by calcium, Me_2SO or other treatments, appears to result from conditions that lower the free energy of the compacted lipid multilayer structure. The intramembrane particles behave as if they are floating in the central oily stratum of the lipid bilayer with projections or connections extending into the aqueous spaces beyond the lipid polar groups. To bring the surfaces of facing bilayers together, the protein particles must be squeezed out of the way. The lateral displacement of the particles can be driven by attraction of the lipid surfaces for each other. Calcium, tetracaine and other divalent cations presumably bring bilayers together by binding with higher affinity to the acidic lipids of closely apposed bilayers than to these groups in separated surfaces.

The ratio of the membrane surface in close-packed particle-free layers to that of the protein-enriched domains depends on the energy balance. As the protein particles are crowded closer together, the energy will increase until it just offsets the decrease in free energy from bringing bilayer surfaces together. With calcium and tetracaine at concentrations above the critical level, diffraction from the protein-enriched phase eventually disappears. Micrographs of freeze-fractured specimens show that the particles are eventually packed in domains that occupy a small fraction of the membrane surface. Disappearance of measurable diffraction from these protein-enriched domains could be due to lack of scattering contrast between layers if the protein is fairly uniform in cross-section and if there is relatively little lipid still associated with the protein. Increased disorder in protein-enriched layers would also lead to reduced coherent diffraction.

Kinetics

Compaction of myelin by calcium is very slow compared to the relatively rapid transformation produced by Me_2SO and by tetracaine. Differences in the rate of action correlate with the permeability of the tissue to each agent. Lipid membranes are more permeable to local anesthetics [51] and Me_2SO [52] than to calcium [53].

In order to induce switching to the compacted state, divalent cations must penetrate the sheath and build up to the critical level of about 10 mM. The time required to reach the critical concentration inside the nerve is diminished as the outside concentration increases. Higher temperatures also accelerate the transformation, presumably by facilitating permeation. At low concentrations, Me_2SO complements the action of calcium by lowering the threshold for compaction.

Permeability barriers may exist at several levels within the tissue. Myelin in brain white matter is transformed more rapidly than that in sciatic nerves; and removal of the perineural connective tissue sheath of frog sciatic nerve hastens the compacting action of calcium.

Transition from the normal period array to the compacted form of myelin proceeds through intermediate states that may be quite disordered. The process is similar to the transition induced by Me_2SO except that the time scale is greatly expanded. At high calcium concentrations (100 mM), the initial large decrease in the coherent diffracting power and increase in incoherent scattering

means that the normal period array becomes disordered before the compaction occurs. At lower concentrations (33 mM), the disordering of the normal myelin structure proceeds more gradually and, in a number of tissues, a transient 147 Å period structure is observed. This is presumably an intermediate state in the formation of the 126 Å period compacted phase.

When diffraction from the compacted phase reaches a stable intensity, its diffracting power is comparable to that of the normal myelin before treatment. Most of the scattering density contrast of the various states of myelin membranes is due to the lipid bilayer. The intensity measurements indicate that most of the myelin lipids end up in the compacted particle-free layers.

Asymmetry of the compacted layers is evident both from the electron micrographs and X-ray patterns that show a pair of membranes in the 126 Å repeat. With time, the intensity of the odd-order reflections from the compacted phase weakens and disappears. This indicates that there is rearrangement of the lipid (and residual proteins) to form a symmetric bilayer. Rearrangement into symmetric bilayers takes only a few hours with 20 mm tetracaine, but it takes several days with 100 mM calcium.

Myelin breakdown and membrane fusion

The vesiculation and rearrangement seen in thin-sectioned calcium- and tetracaine-treated myelin at late stages of compaction (Figs. 1b and 5) have not been observed with nerves compacted by dehydrating treatments and prepared in the same way for electron microscopy. Disruption of the continuity of myelin membranes is not, therefore, a necessary consequence of compaction. Vesiculation may arise from fusion of multilayer domains following charge neutralization, similar to the fusion mechanism for acidic lipid disperions. The vesiculation of calcium- and tetracaine-treated myelin seen in freeze-fracture, however, may represent a further structural deterioration due to the action of cryoprotectants on the close-packed membranes.

Disruption of the myelin sheath may cause irreversible loss of conductivity in calcium-treated nerves. Lorente de Nó [54] observed that extended exposure to calcium at concentrations of 10—50 mM selectively impaired conduction by myelinated A fibers while unmyelinated C fibers recovered conductivity when returned to normal Ringer's solution. This loss of conductivity in calcium-treated nerves correlates with the occurrence of irregular swelling and breaking of the myelin sheaths visible by light microscopy.

Reorganization of the myelin sheath following treatment with calcium or tetracaine may result from fusion of closely apposed membrane bilayers. In secretory systems, the close contact of apposing membranes that precedes fusion may be stabilized by divalent cations, but fusion itself is a highly specific event usually involving calcium-activated proteins. In neuromuscular junctions, high concentrations of divalent cations (50 mM) stabilize close contact of synaptic vesicles with presynaptic membranes, but contact under these conditions does not lead to fusion [1,2]. These membrane interactions probably depend on the same ionic forces that act in myelin. Our observations do not explain the ways that myelin breaks down; but the correlation of the effects of calcium and tetracaine on myelin and on myelin lipids does provide information about the forces between membrane layers and the role of the intrinsic membrane proteins in stabilizing the normal periodic arrangement.

Acknowledgements

We thank Drs. N.P. Franks and D.A. Kirschner for advice and helpful information; Dr. W.C. Phillips for assistance with the diffraction experiments; Dr. L. Makowski and Ms. M. Haghooie for assistance in data processing; Dr. D.A. Goodenough for use of his facilities for freeze-fracture; Dr. D.L. Melchior and Mr. F. Scavitto for measuring the partial specific volume of myelin lipids; Ms. M. Cahoon for specimen preparation and analysis; and Mr. W. Saunders for photography. This work was supported by U.S. Public Health Service grants NS 14378 and NS 13408 (to D.A. Kirschner) from the National Institute of Neurological and Communicative Disorders and Stroke, CA 15468 from the National Cancer Institute, and National Science Foundation grant PCM 77-16271 from the Human Cell Biology Program.

References

1 Heuser, J.E. (1977) in Depolarization-Release Coupling Systems in Neurons (Llinas, R.R. and Heuser, J.E., eds.) Neurosci. Res. Prog. Work Sessions, 1975 and 1976, Neurosci. Res. Prog. Bull., Vol. 15, pp. 631—635, MIT Press, Cambridge
2 Boyne, A.F., Bohan, T.P. and Williams, T.H. (1974) J. Cell Biol. 63, 780—795
3 Schober, R., Nitsch, C., Rinne, U. and Morris, S.J. (1977) Science 195, 495—497
4 Palmer, K.J. and Schmitt, F.O. (1941) J. Cell. Comp. Physiol. 17, 385—394
5 Ahkong, Q.F., Fisher, D., Tampion, W. and Lucy, J.A. (1975) Nature 253, 194—195
6 Lawson, D., Raff, M.C., Gomperts, B., Fewtrell, C. and Gilula, N.B. (1977) J. Cell Biol. 72, 242—259
7 Jacobson, K. and Papahadjopoulos, D. (1975) Biochemistry 14, 152—161
8 Lansman, J. and Haynes, D.H. (1975) Biochim. Biophys. Acta 394, 335—347
9 Papahadjopoulos, D., Vail, W.J., Pangborn, W.A. and Poste, G. (1976) Biochim. Biophys. Acta 448, 265—283
10 Worthington, C.R. and McIntosh, T.J. (1976) Biochim. Biophys. Acta 436, 707—718
11 Kirschner, D.A. and Caspar, D.L.D. (1975) Proc. Natl. Acad. Sci. U.S. 72, 3513—3517
12 Benitez, D., Caspar, D.L.D. and Kirschner, D.A. (1977) in Proc. Electron Microscopy Soc. Am., Boston, 1977, Vol. 35, pp. 600—601, Claitors Publishing Division, Baton Rouge
13 Norton, W.T. and Poduslo, S.E. (1973) J. Neurochem. 21, 749—757
14 Folch, J., Lees, M. and Sloane-Stanley, G.H. (1957) J. Biol. Chem. 226, 497—509
15 Lees, M.B. (1968) J. Neurochem. 15, 153—159
16 Rouser, G., Kritchevsky, G., Yamamoto, A., Simon, G., Galli, C. and Bauman, A.J. (1969) Methods Enzymol. 14, 272—317
17 Bailey, J.L. (1967) Techniques in Protein Chemistry, pp. 340—341, Elsevier, Amsterdam
18 Marinetti, G.V. (1962) J. Lipid Res. 2, 1—20
19 Searcy, R.L. and Bergquist, L.M. (1960) Clin. Chim. Acta 5, 192—199
20 Svennerholm, L.J. (1956) J. Neurochem. 1, 42—53
21 Kinsky, S.C. (1974) Methods Enzymol. 32, 501—513
22 Pinto da Silva, P. and Miller, R.G. (1975) Proc. Natl. Acad. Sci. U.S. 72, 4046—4050
23 Feng, T.P. and Liu, Y.M. (1949) J. Cell. Comp. Physiol. 34, 1—16
24 Frankenhaeuser, B. (1957) J. Physiol. 137, 245—260
25 Feinstein, M.B. (1964) J. Gen. Physiol. 48, 357—374
26 Caspar, D.L.D. and Phillips, W.C. (1976) in Neutron Scattering for the Analysis of Biological Structures (Schoenborn, B.P., ed.), Brookhaven Symp. Biol., Upton, 1975, Vol. 27, pp. VII-107—VII-125, Brookhaven National Laboratory, Upton
27 Blaurock, A.E. and Nelander, J.C. (1976) J. Mol. Biol. 103, 421—431
28 Nelander, J.C. and Blaurock, A.E. (1978) J. Mol. Biol. 118, 497—532
29 Kirschner, D.A. (1974) in Spectroscopy in Biology and Chemistry (Yip, S. and Chen, S.-H., eds.), pp. 203—233, Academic Press, New York
30 Franks, N.P. (1976) J. Mol. Biol. 100, 345—358
31 Rand, R.P. and Luzzati, V. (1968) Biophys. J. 8, 125—137
32 Worcester, D.L. and Franks, N.P. (1976) J. Mol. Biol. 100, 359—378
33 Melchior, D.L., Scavitto, F.J., Walsh, M.T. and Steim, J.M. (1977) Thermochim. Acta 18, 43—71
34 Gregson, N.A. (1976) in The Peripheral Nerve (Landon, D.N., ed.), pp. 512—604, Chapman and Hall, London

35 Braun, P.E. and Brostoff, S.W. (1977) in Myelin (Morell, P., ed.), pp. 201—231, Plenum Press, New York
36 Braun, P.E. (1977) in Myelin (Morell, P., ed.), pp. 91—115, Plenum Press, New York
37 Caspar, D.L.D. and Kirschner, D.A. (1971) Nat. New Biol. 231, 46—52
38 Schmitt, F.O. and Bear, R.S. (1939) Biol. Rev. 14, 27—50
39 Melchior, D.L. and Steim, J.M. (1976) Annu. Rev. Biophys. Bioeng. 5, 205—238
40 Luzzati, V. and Husson, F. (1962) J. Cell Biol. 12, 207—219
41 Luzzati, V. (1968) in Biological Membranes (Chapman, D., ed.), Vol. I, pp. 71—123, Academic Press, New York
42 Wilkins, M.H.F., Blaurock, A.E. and Engelman, D.M. (1971) Nat. New Biol. 230, 72—76
43 Esfahani, M., Limbrick, A.R., Knutton, S., Oka, T. and Wakil, S.J. (1971) Proc. Natl. Acad. Sci. U.S. 68, 3180—3184
44 Ladbrooke, B.D., Jenkinson, T.J., Kamat, V.B. and Chapman, D. (1968) Biochim. Biophys. Acta 164, 101—109
45 Ladbrooke, B.D., Williams, R.M. and Chapman, D. (1968) Biochim. Biophys. Acta 150, 333—340
46 Cowley, A.C., Fuller, N.L., Rand, R.P. and Parsegian, V.A. (1978) Biochemistry 17, 3163—3168
47 Barton, P.G. (1968) J. Biol. Chem. 243, 3884—3890
48 Abramson, M.B., Katzman, R. and Curci, R. (1965) J. Colloid Sci. 20, 777—787
49 Abramson, M.B., Colacicco, G., Curci, R. and Rapport, M.M. (1968) Biochemistry 7, 1692—1698
50 McLaughlin, S.G.A., Szabo, G. and Eisenman, G. (1971) J. Gen. Physiol. 58, 667—687
51 Seeman, P. (1972) Pharmacol. Rev. 24, 583—655
52 Jacob, S.W., Bischel, M. and Herschler, R.J. (1964) Curr. Ther. Res. 6, 193—198
53 Vanderkooi, J.M. and Martonosi, A. (1971) Arch. Biochem. Biophys. 147, 632—646
54 Lorente de Nó, R. (1947) Stud. Rockefeller Inst. Med. Res. 131, 122—126